<Original Paper> Journal of the Korean Society for Nondestructive Testing, Vol. 36, No. 2: 102-111, 2016
ISSN 1225-7842 / eISSN 2287-402X *http://dx.doi.org/10.7779/JKSNT.2016.36.2.102*

# An Efficient and Accurate Method for Calculating Nonlinear Diffraction Beam Fields

Hyunjo Jeong*†, Sungjong Cho*, Kiwoong Nam* and Janghyun Lee*

**Abstract** This study develops an efficient and accurate method for calculating nonlinear diffraction beam fields propagating in fluids or solids. The Westervelt equation and quasilinear theory, from which the integral solutions for the fundamental and second harmonics can be obtained, are first considered. A computationally efficient method is then developed using a multi-Gaussian beam (MGB) model that easily separates the diffraction effects from the plane wave solution. The MGB models provide accurate beam fields when compared with the integral solutions for a number of transmitter-receiver geometries. These models can also serve as fast, powerful modeling tools for many nonlinear acoustics applications, especially in making diffraction corrections for the nonlinearity parameter determination, because of their computational efficiency and accuracy.

**Keywords:** Nonlinear Beam Field, Quasilinear Theory, Integral Solution, Multi-Gaussian Beam, Diffraction

## 1. Introduction

Nonlinear acoustics is widely applied for the purpose of characterizing damage states and material properties in solids and fluids. The acoustic nonlinearity parameter is one of the quantitative indicators that is known to be more sensitive to certain damages and material states than traditional linear parameters such as velocity, attenuation. For solids, acoustic nonlinearity has been used to characterize material damage and microstructural changes [1-3]. For fluids, studies of acoustic nonlinearity were mainly focused to harmonic imaging of biological tissues [4,5]. In water, acoustic nonlinearity plays an important role in the development of parametric arrays for underwater sonar imaging [6].

The finite amplitude method is the most widely used technique for determination of the acoustic nonlinearity parameter $\beta$ of solids and fluids. In general, the propagation of a finite-amplitude plane wave through a nonlinear medium introduces distortions, resulting in the generation of higher harmonics. The nonlinearity parameter $\beta$ is based on the plane wave solution of nonlinear wave equation, and is determined from the ratio of amplitudes of the fundamental and that of the second harmonic generated in the medium [7]. However, the plane wave assumption generally does not hold in reality, therefore beam diffraction effects should be taken into account for accurate determination of nonlinearity parameter.

The purpose of this study is to develop an efficient and precise modeling technique for calculating nonlinear diffraction beam fields. The model developed here will be extended further to derive and then apply explicit diffraction corrections for accurate determination of the nonlinearity parameter in fluids or solids. The second part will be published in a separate companion paper [8]. Attenuation effects are not considered in this study, and will be studied in a separate paper.

We need a three-dimensional nonlinear equation to predict the actual acoustic behavior

[Received: February 2, 2016, Revised: April 2, 2016, Accepted: April 5, 2016] *Division of Mechanical and Automotive Engineering, Wonkwang University, Iksan 54538, Jonbuk Korea †Corresponding Author: hjjeong@wku.ac.kr

frequently encountered in typical finite amplitude experiments for harmonic generation. The model equation should be able to account for nonlinearity and diffraction. For this purpose, the Westervelt equation [9,10] is used in this study. It is described in three dimensional coordinates, as opposed to the two cylindrical coordinates of the Khokholov-Zabolotskaya-Kuznetsov (KZK) equation [9]. Moreover, its linear equation yields the Rayleigh-Sommerfeld integral [10], which is valid for all axial ranges. The first order KZK solution, however, is not valid for small axial distances $z \le a(ka)^{1/3}$ [11]. Recently, the Westervelt equation was used to calculate the difference frequency fields of a parametric array [10].

In this work, integral solutions are first derived from the Westervelt equation for the fundamental and second harmonic beam fields based on the quasilinear theory. Multi-layer integral expressions are obtained, and calculations of the acoustic fields are therefore computationally very heavy, especially for the second harmonic. To provide a means for fast calculations of secondary acoustic fields, we employ an approximate analytical model for the primary field with the use of a multi-Gaussian beam (MGB) method. With the use of MGB model in paraxial approximation, the fifth-layer integral of the second harmonic is reduced to a one-dimensional form. The MGB model has been widely used in NDE community for fast and accurate calculations of ultrasonic beam fields radiated from planar or focused transducers. Most of the previous studies on MGB models were limited to linear wave field calculations [12-16]. Labat et al. [17] used the superposition of Gaussian beams to calculate the fundamental and second harmonic fields based on the KZK equation. Here, we extend the MGB model to describe the second harmonic beam fields under the quasilinear and paraxial approximation.

## 2. Westervelt Equation and Quasilinear Solution

To capture the main features of the combined effects of diffraction, and nonlinearity in models of finite amplitude sound beams, one needs theoretical formulations that describe nonlinear acoustic fields in two- or three-dimension. Model equations for sound fields are available with appropriate approximations of the full second-order wave equation [9]. One of such equations is the Westervelt equation. This equation assumes that cumulative nonlinear effects dominate noncumulative (local) nonlinear effects. This assumption is valid in most cases of practical interest. As a general rule, except within one wavelength from the source, local effects can be ignored for problems involving progressive directional sound beams [9].

Neglecting medium absorption, the Westervelt equation is given by

$$\nabla^2 p - \frac{1}{c^2}\frac{\partial^2 p}{\partial t^2} = -\frac{\beta_f}{\rho c^4}\frac{\partial^2 p^2}{\partial t^2} \tag{1}$$

where $p$ is the acoustic pressure, $c$ is the longitudinal sound velocity of fundamental wave, $\rho$ is the density. In Eq. (1), the operator $\nabla^2$ is the Laplacian in the ($x$, $y$, $z$) space, and $z$ is taken as the direction of propagation. The term in the right-hand side describes the effect of acoustic nonlinearity. Thus, the Westervelt equation accounts for the combined effects of diffraction and nonlinearity in progressive directional sound beams. In Eq. (1), $\beta_f$ is the acoustic nonlinearity parameter of fluids, which is given by $\beta_f = -(3 + c_{111}/c_{11})/2$ where $c_{11}$ and $c_{111}$ are the second-order and third-order elastic constants. Eq. (1) can be applicable to isotropic solids with further assumption and by replacing $\beta_f$ with $\beta_s/2$, where $\beta_s$ is the nonlinearity parameter of solids defined by $\beta_s = -(3 + c_{111}/c_{11})$. Hereafter, we shall suppress the subscript $s$.

When nonlinear effects are weak, Eq. (1) can be efficiently solved following the quasilinear theory. The quasilinear solution is assumed to have the form

$$p = p_1 + p_2 \tag{2}$$

where $p_1$ is the linear solution of Eq. (1) for the pressure at a fundamental frequency $\omega$, and $p_2$ is a small correction to $p_1$ at the second harmonic frequency $2\omega$. $|p_2| \ll |p_1|$ is assumed in nonlinear interactions.

Assuming that the pressure is harmonic in time,

$$p_n(\mathbf{x},t) = \mathrm{Re}\left( p_n(\mathbf{x},\omega)\exp(-in\omega t)\right), \quad n = 1,\ 2 \tag{3}$$

where $p_n(\mathbf{x},\omega)$ are complex-valued pressure amplitudes and $\omega$ is the angular frequency of the propagating wave. Substitution of Eqs. (2) and (3) into Eq. (1) yields the following quasilinear system of equations for $p_1(\mathbf{x},\omega)$ and $p_2(\mathbf{x},\omega)$:

$$\nabla^2 p_1 + k^2 p_1 = 0 \tag{4}$$

$$\nabla^2 p_2 + 4k^2 p_2 = \frac{2\beta k^2}{\rho c^2} p_1^2 \tag{5}$$

where $k = \omega/c$ is the wave number of the primary wave. For the source condition, we take

$$p\ (x', y', 0, t) = p_1(x', y', 0, \omega)\exp(-i\omega t) \tag{6}$$

where $p_1(x',y',0,\omega)$ is an arbitrary distribution that takes into account both amplitude and phase. It is also assumed that the source does not radiate at the second-harmonic frequency, that is, $p_2(x',y',0,\omega) = 0$.

Since Eqs. (4) and (5) form Helmholtz equations, the Green's function therefore has to solve these partial differential equations. We define the Green's function $G_n(x,y,z|x',y',z')$ here, at frequency $n\omega$, to be the solution of the following inhomogeneous equation

$$\nabla^2 G_n + (nk)^2 G_n = -\delta(\mathbf{x} - \mathbf{x}') \tag{7}$$

where the right-hand side is the three dimensional Dirac delta function in Cartesian coordinates. Primed coordinates correspond to locations of source points. The Green's function can be obtained as

$$G_1(x,y,z\,|\,x',y',0) = \frac{1}{4\pi r}\exp(ikr) \tag{8}$$

$$G_2(x,y,z\,|\,x',y',z') = \frac{1}{4\pi R}\exp(i2kR) \tag{9}$$

where $r = \sqrt{(x-x')^2 + (y-y')^2 + z^2}$ and $R = \sqrt{(x-x')^2 + (y-y')^2 + (z-z')^2}$.

Solutions of Eqs. (4) and (5) are now obtained by integrating over the product of the Green's function and appropriate source function to sum up the contributions from all source points. For $p_1$, the source function is $p_1(x',y',0,\omega)$, and the integration is performed over the transducer surface elements $ds' = dx'dy'$ in the plane $z' = 0$. The source function for $p_2$ is the right-hand side of Eq. (5), which is proportional to the volume distribution $p_1^2(\mathrm{x}',\omega)$, and the integral is performed over the volume elements $dV' = dx'dy'dz'$. We thus obtain

$$p_1(\mathbf{x},\omega) = -2ik\int_{-\infty}^{+\infty}\int_{-\infty}^{+\infty} p_1(x',y',0)\, G_1(x,y,z\,|\,x',y',0)\, dx'dy' \tag{10}$$

$$p_2(\mathbf{x},\omega) = \frac{2\beta k^2}{\rho c^2}\int_0^z\int_{-\infty}^{+\infty}\int_{-\infty}^{+\infty} p_1^2(x',y',z')\, G_2(x,y,z\,|\,x',y',z')\, dx'dy'dz' \tag{11}$$

The source condition $p_2(x',y',0,\omega) = 0$ establishes the lower integration limit $z' = 0$ in Eq. (11). On the basis of Eq. (11), the second-harmonic generation in the quasilinear approximation is interpreted as a sound field radiated by a volume distribution of virtual sources whose strengths are proportional to $p_1^2(\mathbf{x}')$.

When a constant pressure $p_0(\omega)$ is prescribed over the surface $S'$ of a circular piston transducer of radius $a$, where

$$p_1(x',y',z'=0,\omega)=\begin{cases} p_0(\omega) & x'^2+y'^2\le a^2 \\ 0 & x'^2+y'^2>a^2 \end{cases} \quad (12)$$

Substitution of Eq. (8) into Eq. (10) provides the Rayleigh-Sommerfeld (RS) integral [14]

$$p_1(\mathbf{x},\omega)=-\frac{ikp_0}{2\pi}\int_{-\infty}^{+\infty}\int_{-\infty}^{+\infty}\frac{\exp(ikr)}{r}\,dx'dy' \quad (13)$$

The RS integral is the exact solution to the linear wave equation, Eq. (4), and represents the transducer radiation as a superposition of spherical waves radiating from point sources distributed on the plane $z'=0$.

Similarly, substitution of Eq. (9) into Eq. (11) yields the quasilinear solution for the second harmonic pressure

$$p_2(\mathbf{x},\omega)=\frac{\beta k^2}{2\pi\rho c^2}\int_0^z\int_{-\infty}^{+\infty}\int_{-\infty}^{+\infty}p_1^2(x',y',z')\,\frac{\exp(i2kR)}{R}\,dx'dy'dz' \quad (14)$$

The Green's function used in this integral includes contribution of the element $dV'=dx'dy'dz'$ of the virtual source formed by the primary field. Eq. (14) also serves as an exact solution to the second harmonic wave equation in the quasilinear theory since the exact linear solution $p_1$ is used in the right hand-side of Eq. (11) to calculate an additional pressure perturbation due to nonlinearity.

Eq. (14) for calculation of $p_2$ together with Eq. (13) represents the fifth-fold integral that is very time consuming to be calculated numerically. For this reason, an approximate analytic solution of integral (14) is needed under the high-frequency approximation of primary field. For this purpose, a multi-Gaussian beam (MGB) model can be employed as an efficient alternative method for accurate numerical calculations.

## 3. Multi-Gaussian Beam(MGB) Models

Multi-Gaussian beam (MGB) models have been widely used to describe the propagation of ultrasonic beams from planar or focused transducers [12-16]. One of the attractive features of MGB models is that they are numerically very efficient. This is because these models rely on the superposition of a small number (15-25) of Gaussian beams whose properties can be described in analytical terms.

Another feature of MGB models, as will be seen later, is that they provide closed form solutions for diffraction corrections. Since the Westervelt equation and the quasilinear theory provide integral solutions, it is not easy to separate diffraction effects from the plane wave solution. With MGB models, however, the effects of diffraction of the nonlinear acoustic fields, as they travel from the source transducer to the receiver transducer, can be obtained explicitly. Most of the previous studies on MGB models were limited to linear wave field calculations. Here, we extend the MGB model to describe the second harmonic wave fields.

According to Wen and Breazeale[18], on the face of transducer of radius a located at the plane $z'=0$, the pressure field can be approximated by a sum of Gaussians

$$p_1(x',y',0)=\sum_{m=1}^{N}p_0A_m\exp(-B_m(x'^2+y'^2)/a^2) \quad (15)$$

where $p_0$ is the constant pressure on the transducer surface, and $A_m$ and $B_m$ are a set of complex-valued expansion coefficients [18-20].

If we assume that $ka\gg 1$, the beam is reasonably directional and localized in the vicinity of the z axis, the Green's function in Eq. (8) can be simplified into the paraxial approximation as

$$\frac{\exp(ikr)}{r}\approx\frac{1}{z}\exp\left[(ik)\left\{z+\frac{(x-x')^2}{2z}+\frac{(y-y')^2}{2z}\right\}\right] \quad (16)$$

Substitution of Eqs. (15) and (16) into Eq. (13), after some algebra with the use of a known integral formula,

$$\int_{-\infty}^{+\infty} \exp\left(-ax^2+bx\right)dx = \sqrt{\frac{\pi}{a}}\exp\left(\frac{b^2}{4a}\right), \tag{17}$$

will yield the MGB model for the primary beam field given by

$$p_1(\mathbf{x},\omega) = \sum_{m=1}^{N} \frac{p_0 A_m \exp(ikz)}{1+iB_m z/D_R} \exp\left(\frac{i\omega}{2}\frac{iB_m/cD_R}{1+iB_m z/D_R}(x^2+y^2)\right) \tag{18}$$

where $D_R = ka^2/2$ is the Rayleigh distance. Eq. (18) can be rearranged to be written in the form

$$p_1(\mathbf{x},\omega) = \left[p_0\exp(ikz)\right]\left[\sum_{m=1}^{N}\frac{A_m}{1+iB_m z/D_R}\exp\left(\frac{i\omega}{2}\frac{iB_m/cD_R}{1+iB_m z/D_R}(x^2+y^2)\right)\right] \tag{19}$$

where the first term represents the fundamental pressure of a pure plane wave, the second term the diffraction correction term.

Now substitution of Eq. (19) into Eq. (14), after some algebra, provides the MGB model for the second harmonic beam field

$$p_2(\mathbf{x},\omega) = \frac{\beta k p_0^2}{\rho c^2}\int_0^z \sum_{m=1}^{N}\sum_{n=1}^{N}\frac{A_m A_n \exp(2ikz)}{(2+B_a z)+(B_a-2B_b z)z'}\times \exp\left\{ik(x^2+y^2)\left(\frac{B_a-2B_b z'}{(2+B_a z)+(B_a-2B_b z)z'}\right)\right\}dz' \tag{20}$$

where $B_a = i(B_m+B_n)/D_R; B_b = B_m B_n/D_R^2$.

With the use of paraxial approximation in the MGB model for the primary field, the fifth-layer integral representation of the second harmonic wave field, Eq. (14), is now reduced to a one-dimensional form. Therefore, the computation time will be greatly reduced, as will be seen later.

In a similar manner to Eq. (19), Eq. (20) can also be written in the form of a plane wave modified by diffraction correction

$$p_2(\mathbf{x},\omega) = \left[\frac{\beta k p_0^2 z}{2\rho c^2}\exp(2ikz)\right]\times \left[\frac{1}{z}\int_0^z \sum_{m=1}^{N}\sum_{n=1}^{N}\frac{2A_m A_n}{(2+B_a z)+(B_a-2B_b z)z'}\exp\left\{ik(x^2+y^2)\left(\frac{B_a-2B_b z'}{(2+B_a z)+(B_a-2B_b z)z'}\right)\right\}dz'\right] \tag{21}$$

where the first term represents the second harmonic pressure of the pure plane wave. We define the second term as a diffraction correction of the paraxial MGB model for the second harmonic wave.

## 4. Simulation Results and Computational Efficiency

The accuracy of MGB models [Eqs. (18) and (20)] can be tested by comparing with the exact solutions obtained from the RS integral [Eqs. (13) and (14)]. The acoustical field variable used in these equations is pressure. We change this variable to particle displacement following the relationship:

$$p_n = -in\rho c\omega u_n, \quad n=1,\ 2 \tag{22}$$

In all subsequent calculations and measurements, the particle displacements will be used as acoustical field variables.

To calculate the received displacement at a distance $z$ by a circular transducer of radius b, the concept of average displacement will be used and calculated as follows:

$$u_n(z) = \frac{1}{\pi b^2}\int_0^b u_n(r,z)\ 2\pi r\,\mathrm{d}r, \quad n=1,2 \tag{23}$$

where $u_n(r,z)$ is computed from Eq. (22) and $r=\sqrt{x^2+y^2}$.

For simulation, consider a piston transducer of $2a$=9.5 mm diameter radiating into water at 3.5 MHz, where a denotes the radius of the transmitting transducer. The properties of water used are: c=1480 m/s, $\rho$=1000 kg/m$^3$, $\beta$=3.5. The initial displacement amplitude used is $u_0 = 10^{-9}$ m. Comparisons were first made for

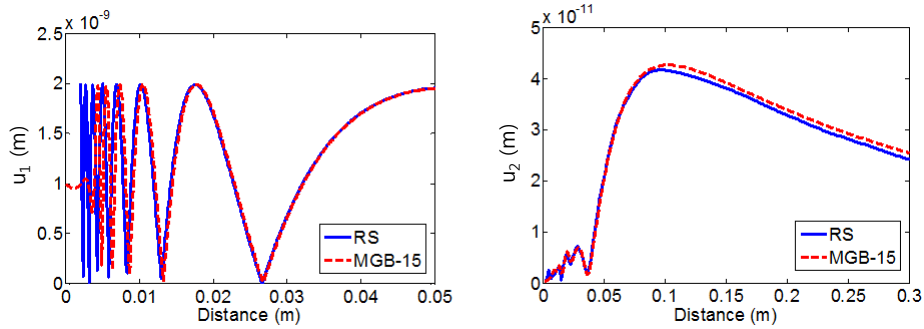


(a) (b)

Fig. 1 On-axis beam fields calculated as a function of propagation distance by RS integral solutions and MGB models: (a) fundamental displacement amplitude $u_1$, and (b) second harmonic displacement amplitude $u_2$. *N*=15 expansion coefficients were used in the MGB model calculations.

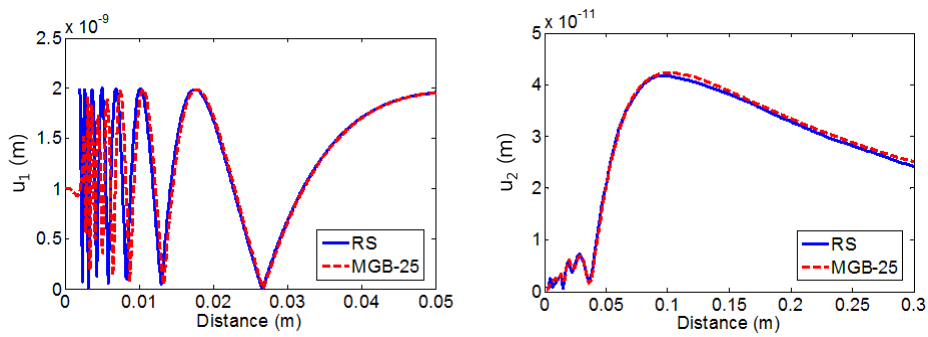


(a) (b)

Fig. 2 On-axis beam fields calculated as a function of propagation distance by RS integral solutions and MGB models: (a) fundamental displacement amplitude $u_1$, and (b) second harmonic displacement amplitude $u_2$. *N*=25 expansion coefficients were used in the MGB model calculations.

on-axis displacement amplitudes to be received by a point receiver. The number of expansion coefficients for $A_n$ and $B_n$ used in the MGB model are known to have effects on the beam field of the fundamental wave in the very near field. Kim et al. [19] obtained better results with a larger number (25 Gaussians) of expansion coefficients. The second harmonic beam field will also be affected by the fundamental wave. Therefore, two different numbers of expansion coefficients were tested: $N$ = 15 and 25. These coefficients are listed in [20] and [19].

Fig. 1(a) shows the results of using 15 expansion coefficients in the MGB model to calculate the on-axis displacement amplitudes of the fundamental wave, and compares with the results calculated exactly by using the RS integral solution. The multi-Gaussian beam model accurately models the on-axis linear displacement field of the transducer down to approximately 5 mm from the transduce face. Fig. 1(b) shows a similar comparison for the on-axis second harmonic displacement field. The MGB model starts to show deviation from the exact displacements after passing the near-field distance, and this deviation remains fairly constant thereafter.

Fig. 2(a) shows the results of using 25 expansion coefficients to calculate the on-axis displacement field where now the MGB model

is accurate to distance from the transducer of approximately 3 mm or greater. Use of the 25 expansion coefficients also give better agreement over 15 coefficients for the second harmonic displacement field, as shown in Fig. 2(b). Therefore, all subsequent MGB model calculations will be done using 25 expansion coefficients.

The MGB model is an approximate paraxial solution to the linear wave equation, so that it cannot accurately model the fundamental field in the very near field from the transducer in case of a point receiver. The paraxial approximation used in the MGB model of the fundamental field also influences the accuracy of the MGB model of the second harmonic field because it is used as a forcing function for the second

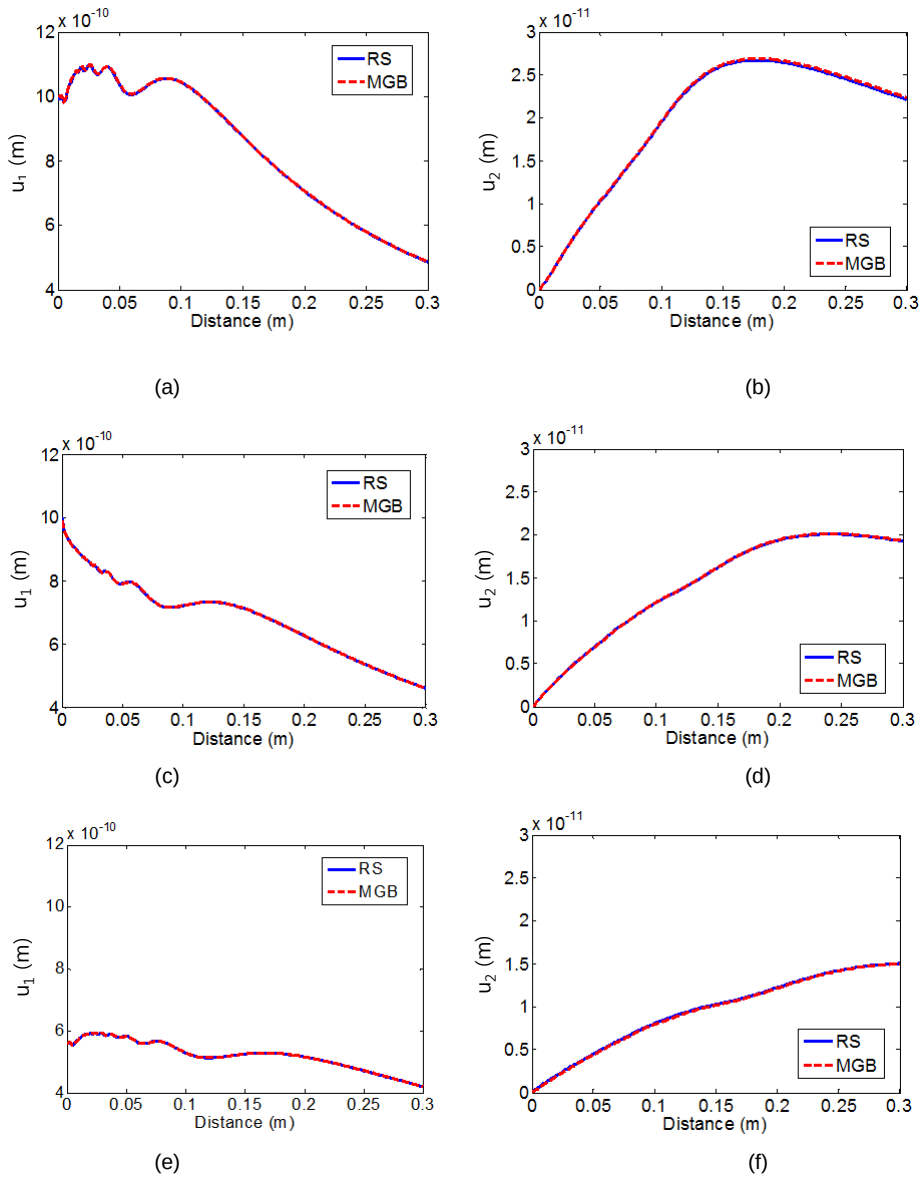


Fig. 3 Average displacement amplitudes calculated by RS integral solutions and MGB models for different transmitter and receiver sizes: (a), (b) 2a=9.5 mm, 2b=6.35 mm, (c), (d) 2a=9.5 mm, 2b=9.5 mm, and (e), (f) 2a=9.5 mm, 2b=12.7 mm. Figures in the left column represent the fundamental displacement amplitudes, while figures in the right column represent the second harmonic displacement amplitudes.

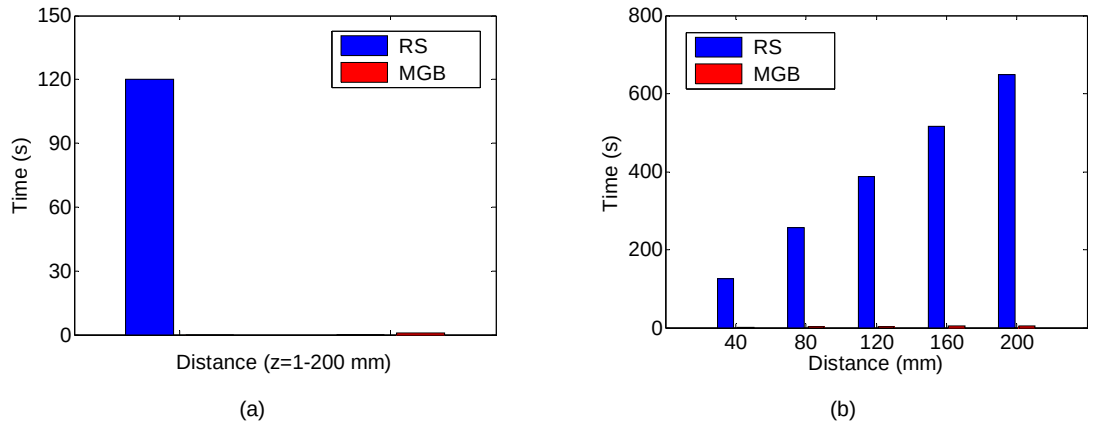


Fig. 4 A Comparison of computation times for the average displacement amplitudes calculated by the MGB models and by the RS integrals solutions when the size of transmitter and receiver is the same, 2a=2b= 9.5 mm: (a) total time to calculate the average displacements of the fundamental wave from distance z=1 to 200 mm, and (b) time to calculate the average displacements of the second harmonic wave at several selected distances

harmonic generation. The point receiver here can be regarded as an ideal case not encountered in common ultrasonic testing. As can be seen in further simulations below, the effect of paraxial approximation is negligible in cases of finite size receivers, and the overall agreement of MGB model with the exact solution is pretty good.

Fig. 3 shows the average displacement amplitudes calculated by the RS integral solutions and MGB models for different combinations of transmitter and receiver sizes. Compared to the oscillatory behavior of the fundamental and the second harmonic of a point receiver in Figs. 1 and 2, the averaging over the receiver tends to smooth much of the oscillatory behavior in the near field. Both of the fundamental and the second harmonic displacements calculated by the MGB model agree well with the exact displacements for the most part of the range covered. Based on these comparisons with exact solutions, the paraxial MGB model can be used as a practical, accurate modeling tool for many nonlinear acoustics problems.

The efficiency of the MGB model in terms of computation time was also tested. Fig. 4 shows a comparison of computation times for the average displacement amplitudes as calculated by the MGB models and the method of RS integrals when the transmitting and receiving transducers are the same size, $2a$=$2b$= 9.5 mm.

The fundamental displacement field at any point in the space, $u_1(x,y,z)$, is calculated exactly by using the Rayleigh-Sommerfeld integral Eq. (13). This integral requires discretization of the source transducer area into many small elements, and then performs area integrations using the appropriate Green's functions. The MGB model, on the other hand, calculates the fundamental displacement field, without any integration, just doing summations over the Gaussian beam expansion coefficients Eq. (18). In comparison of example calculations shown in Fig. 4(a), the MGB model is found to be more than one order of magnitude faster than the RS integral.

For the second harmonic field calculation, the RS integral requires fifth-fold integration. The primary displacement calculated above now serves as virtual source, $u_1(x',y',z')$, for the second harmonic generation. This is carried out for all points in a circular slice of the region

parallel to the transducer plane. These primary displacements are then squared and, using the appropriate Green's functions, propagated onto the target point. This is then repeated for all slices of the region, and the contributions from all slices are summed Eq. (14). Consequently, this integration process will require a lot of computation time. On the other hand, the MGB model needs one-dimensional integration with discretization of small line elements in the $z$ direction only Eq. (20), so it is at least two orders of magnitude more numerically efficient than a direct numerical evaluation of a RS integral calculation of the secondary wave field Fig. 4(b).

## 5. Summary and Future Work

In this work, we developed an analytical method to calculate diffraction beam fields of nonlinear waves propagating in fluids or solids. We employed the Westervelt equation as an analytical model that takes into account the combined effects of diffraction and nonlinearity. The quasilinear approximation was then used to predict the finite amplitude sound beam radiated by a plane piston source. Based on the integral expressions of the fundamental and second harmonics of the quasilinear theory, the paraxial multi-Gaussian beam (MGB) model was developed. It describes precisely the fundamental and second harmonic beam fields, and computationally very efficient. Another nice property of the MGB model is that the wave field of a transducer can be written as a plane wave propagation term modified by a diffraction correction term. Future work will include extension of the MGB model to derive explicit diffraction corrections for accurate determination of the nonlinearity parameter in fluids or solids. Attenuation effects are another factor to be considered in nonlinearity parameter evaluation.

## Acknowledgements

This work was supported by Basic Science Research Program through the National Research Foundation of Korea (NRF) funded by the Ministry of Science, ICT & Future Planning (Grant No. 2013-M2A2A9043241 and 2013-R1A2A2A01016042).

## References

[1] A. Kumar, C. J. Torbet, J. W. Jones and T. M. Pollock, "Nonlinear ultrasonics for in situ damage detection during high frequency fatigue," *J. Appl. Phys.*, Vol. 106, 024904 (2009)

[2] J.-Y. Kim, L. J. Jacobs, J. Qu and J. W. Littles, "Experimental characterization of fatigue damage in a nickel-base superalloy using nonlinear ultrasonic waves," *J. Acoust. Soc. Am.*, Vol. 120, pp. 1266-1273 (2006)

[3] J. H. Cantrell, "Substructural organization, dislocation plasticity and harmonic generation in cyclically stressed wavy slip metals," *Proc. Royal Soc. London Series A - Math. Phys. Eng. Sci.*, Vol. 460, pp. 757-780 (2004)

[4] K. D. Wallace, C. W. Lloyd, M. R. Holland and J. G. Miller, "Finite amplitude measurements of the nonlinear parameter B/A for liquid mixtures spanning a range relevant to tissue harmonic mode," *Ultrasound Med. Biol.*, Vol. 33, pp. 620-629 (2007)

[5] L. Bjorno, "Characterization of biological media by means of their nonlinearity," *Ultrasonics*, Vol. 24, pp. 254-259 (1986)

[6] F. Prieur, S. P. Nasholm, A. Austeng, F. Tichy and S. Holm, "Feasibility of second harmonic imaging in active sonar: measurements and simulations," *IEEE J. Oceanic Eng.*, Vol. 37, pp. 467-477 (2012)

[7] L. K. Zarembo and V. A. Krasil'nikov, "Nonlinear phenomena in the propagation of elastic waves in solids," *Sov. Phys. Uspekhi*, Vol. 13, pp. 778-797 (1971)

[8] H. Jeong, S. Cho, K. Nam and J. Lee, "Diffraction corrections for second harmonic beam fields and effects on the nonlinearity parameter evaluation," *Journal of the Korean Society for Nondestructive Testing*, Vol. 36, No. 2, pp. 112-120 (2016)

[9] M. F. Hamilton and C. L. Morfey, "Model Equations," Nonlinear Acoustics, M. F. Hamilton and D. T. Blackstock, Eds., Academic Press, San Diego, USA, pp. 41-63 (2008)

[10] M. Cervenka and M. Bednarik, "Non-paraxial model for a parametric acoustic array," *J. Acoust. Soc. Am.*, Vol. 134, pp. 933-938 (2013)

[11] S. R. Best, A. J. Croxford and S. A. Neild, "Modelling harmonic generation measurements in solids," *Ultrasonics*, Vol. 54, pp. 442-450 (2014)

[12] X. Zhao and T. Gang, "Nonparaxial multi-Gaussian beam models and measurement models for phased array transducers," *Ultrasonics*, Vol. 49, pp. 126-130 (2009)

[13] H. Jeong and L. W. Schmerr, Jr., "Ultrasonic transducer fields modeled with a modular multi-Gausssian beam and application to a contact angle beam testing," *Research in Nondestructive Evaluation*, Vol. 19, pp. 87-103 (2008)

[14] L. W. Schmerr Jr. and S.-J. Song, "Ultrasonic Nondestructive Evaluation Systems - Models and Measurements," Springer, New York, USA, pp. 179-234 (2007)

[15] H. Jeong, M.-C. Park and L. W. Schmerr, Jr., "Application of a modular multi-Gaussian beam model to ultrasonic wave propagation with multiple interfaces," *Journal of the Korean Society for Nondestructive Testing*, Vol. 25, pp. 163-170 (2005)

[16] H. Jeong and L. W. Schmerr, Jr., "Effects of material anisotropy on ultrasonic beam propagation: Diffraction and beam skew," *Journal of the Korean Society for Nondestructive Testing*, Vol. 26, pp. 198-205 (2006)

[17] V. Labat, J. P. Remenieras, O. Bou Matar, A. Ouahabi and F. Patat, "Harmonic propagation of finite amplitude sound beams: experimental determination of the nonlinearity parameter B/A," *Ultrasonics*, Vol. 38, pp. 292-296 (2002)

[18] J. J. Wen and M. A. Breazeale, "A diffraction beam field expressed as the superposition of Gaussian beams," *J. Acoust. Soc. Am.*, Vol. 83, pp. 1752-1756 (1988)

[19] H.-J. Kim, L. W. Schmerr, Jr. and A. Sedov, "Generation of the basis sets for multi-Gaussian ultrasonic beam models-An overview," *J. Acoust. Soc. Am.*, Vol. 119, pp. 1971-1978 (2006)

[20] D. Huang and M. A. Breazeale, "A Gaussian finite-element method for description of sound diffraction," *J. Acoust. Soc. Am.*, Vol. 106, pp. 1771-1781 (1999)